

Stability of the bcc phase of Cu-Al-Mn shape-memory alloys

Eduard Obradó, Lluís Mañosa, and Antoni Planes

*Departament d'Estructura i Constituents de la Matèria, Facultat de Física, Universitat de Barcelona,
Diagonal, 647, E-08028 Barcelona, Catalonia, Spain*

(Received 2 December 1996; revised manuscript received 5 February 1997)

Measurements of the entropy change at the martensitic transition of two composition-related sets of Cu-Al-Mn shape-memory alloys are reported. It is found that most of the entropy change has a vibrational origin, and depends only on the particular close-packed structure of the low-temperature phase. Using data from the literature for other Cu-based alloys, this result is shown to be general. In addition, it is shown that the martensitic structure changes from $18R$ to $2H$ when the ratio of conduction electrons per atom reaches the same value as the eutectoid point in the equilibrium phase diagram. This finding indicates that the structure of the metastable low-temperature phase is reminiscent of the equilibrium structure. [S0163-1829(97)00926-0]

I. INTRODUCTION

It is acknowledged that the stability of bcc metallic phases is controlled by a vibrational entropy associated with a low-lying acoustic transverse phonon branch.¹ Many of these bcc materials undergo a transition to a close-packed structure on cooling. The transition is entropy driven, first order, and diffusionless, and is usually termed a martensitic transformation.² Among the materials undergoing martensitic transformations, Cu-based shape-memory alloys are particularly interesting. These systems belong to the Hume-Rothery class of materials, whose phase stability is largely dominated by the average number of conduction electrons per atom (e/a).³ Commonly, the bcc phase is not stable at moderate temperatures, but it can be retained by means of a suitable cooling treatment. During this cooling the system becomes configurationally ordered. It has recently been shown that ordering can strongly modify the vibrational characteristics of the bcc lattice and, therefore, have an influence on the phase stability of the system.⁴ In addition, the diffusionless nature of the transition ensures that the atom distribution in the high-temperature bcc phase is inherited by the low-temperature close-packed phase, and hence there is no a configurational contribution to the entropy change between the two phases.⁵ Moreover, for these Cu-based alloys the entropic contribution from conduction electrons has been found to be small, and to stabilize the close-packed structure.⁶

In this paper we study the Cu-Al-Mn shape-memory alloy system. This alloy system bears many similarities with traditional Cu-based shape-memory alloys like Cu-Al-Be or Cu-Zn-Al. The important peculiarity that distinguishes Cu-Al-Mn arises from its magnetic properties. While typical shape-memory alloys are diamagnetic, Cu-Al-Mn is paramagnetic at high temperature and undergoes a transition to a magnetic glassy phase at a temperature far below the martensitic transformation.⁷ Such a distinct magnetic behavior could influence the relative stability between the bcc and close-packed phases in Cu-Al-Mn.

In this work we present results of the excess of entropy of the bcc structure for two different families of Cu-Al-Mn alloys; data are compared with published values for other Cu-based systems.

II. EXPERIMENTAL DETAILS

Two families of composition related alloys have been used in the experiments. Their compositions are along the $(\text{Cu}_{0.75}\text{Al}_{0.25})_{1-x}\text{Mn}_x$ ($0.05 \leq x \leq 0.09$), and the $\text{Cu}_3\text{Al}_{1-x}\text{Mn}_{2x}$ ($0.14 \leq x \leq 0.22$) lines. Polycrystalline cylindrical-shaped ingots (5 mm diameter) were obtained by melting pure elements (99.99%). From the ingots, slices (2 mm thick) have been cut using a low-speed diamond saw. The damaged surface has been etched away in a 40% HNO_3 solution. The atomic composition and the measured martensitic transition temperature (on cooling) of each specimen studied are given in Table I.

Calorimetric measurements have been performed using a high-sensitivity microcalorimeter specifically designed to investigate solid-solid phase transitions.⁸ Since this instrument cannot be used at temperatures above room temperature, high-temperature measurements have been carried out in a commercial differential scanning calorimeter. In all cases, prior to a calorimetric measurement, samples have been annealed for 900 s at 1073 K and then quenched into a mixture of ice and water. For sample B1 (which transforms above room temperature) the quench has been performed into boiling water. For all samples, the calorimetric run has been carried out 72 h after the quench.

III. RESULTS AND DISCUSSION

The calorimetric output, proportional to the thermal power (dQ/dt), and the temperature (T) have been simulta-

TABLE I. Atomic composition, average number of valence electrons per atom, and martensitic transition temperatures of the alloys investigated. The first set of alloys belongs to the $\text{Cu}_3\text{Al-Mn}$ line and the second one to the $\text{Cu}_3\text{Al-Cu}_3\text{Mn}_2$ line.

Alloy	at. % Cu	at. % Al	at. % Mn	e/a	M_s (K)
A1	70.09	24.94	4.97	1.499	281
A2	70.09	23.60	6.31	1.472	251
A3	69.29	23.76	6.95	1.475	218
A4	69.21	22.92	7.86	1.458	180
A5	68.22	22.82	8.96	1.456	133
B1	71.23	21.73	7.04	1.435	355
B2	70.89	19.96	9.14	1.399	294
B3	70.40	18.73	10.82	1.375	181

TABLE II. Entropy change of the martensitic transformation obtained 72 h after the thermal treatment, measured on cooling (ΔS_c) and on heating the sample (ΔS_h), and average value (ΔS).

Alloy	$ \Delta S_c $ (J/mol K)	ΔS_h (J/mol K)	ΔS (J/mol K)
A1	1.49	1.43	1.46
A2	1.53	1.57	1.55
A3	1.54	1.52	1.53
A4	1.41	1.32	1.37
A5	1.37	1.11	1.24
B1	1.26	1.21	1.24
B2	1.30	1.33	1.32
B3	1.19	1.20	1.20

neously recorded at a rate of 0.5 Hz. After a proper correction of the base line, the entropy change at the martensitic transformation has been computed as

$$\Delta S = \int_{T_i}^{T_f} \frac{1}{T} \left(\frac{dQ}{dt} \right) \left(\frac{dT}{dt} \right)^{-1} dT, \quad (1)$$

where T_i and T_f are temperatures located, respectively, above (below) and below (above) the start and finishing temperatures on cooling (heating). Results for all the samples investigated are given in Table II. The error associated with ΔS is less than 5%.⁹ Within this experimental uncertainty, no systematic differences between the values for forward and reverse transitions have been obtained. Actually, this is a consequence of the small difference between the heat capacities of the two phases and of a negligible entropy production from irreversible effects at the transition. In the following, the value given for the entropy difference between the bcc and the martensitic phases will correspond to an average over the absolute values obtained in the cooling and heating runs. This quantity will be identified with the excess of entropy of the bcc phase with respect to the corresponding close-packed one. Table II shows that, within the experimental error, the entropy excess data for all the samples studied fall around two different values: $\Delta S = 1.51 \pm 0.05$ J/mol K and $\Delta S = 1.26 \pm 0.06$ J/mol K. The fact that two different values have been obtained suggests the presence of a different product phase for each value of ΔS . Indeed, samples with a low ΔS exhibit a very different thermal spectrum curve than samples with a high ΔS . The different behavior could arise from different martensitic growth mechanisms. The transition for samples with high ΔS has a jerkier character and larger thermal hysteresis than the transition for samples with low ΔS (see Fig. 1). Actually, this different behavior has already been reported for the growth kinetics of the $2H$ (twinning mode mechanism) and the $18R$ (slip mode mechanism) structures.¹⁰ In order to investigate whether different martensitic structures can be found in the samples studied, we have performed x-ray measurements with powders of specimens A1 and B1. The diffractograms are shown in Fig. 2.¹¹ Peaks of the $2H$ phase (γ'_1 phase) are observed in the diffraction pattern corresponding to sample A1, while sample B1 displays peaks of the $18R$ phase (β'_1 phase). There is also a certain amount of residual high-temperature

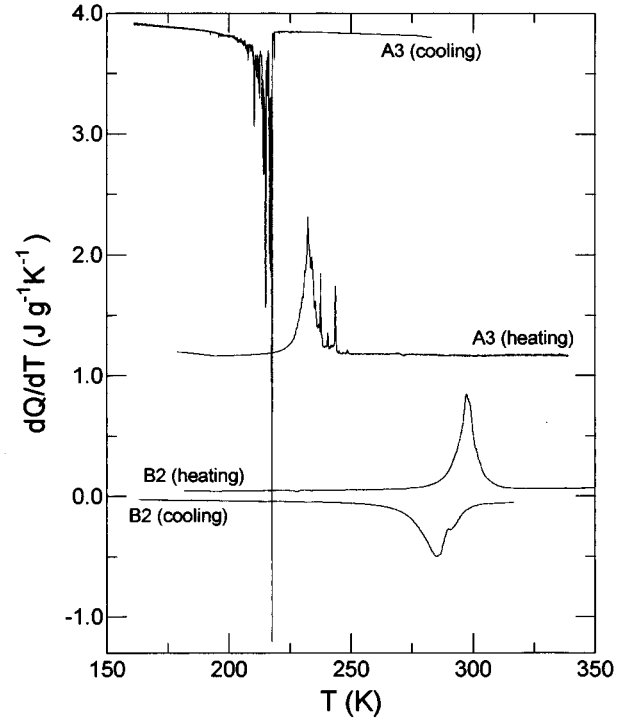


FIG. 1. Typical thermal curves corresponding to the forward (cooling) and reverse (heating) martensitic transformations, obtained 72 h after the heat treatment, for an alloy with $e/a > 1.46$ (sample A3) and for an alloy with $e/a < 1.46$ (sample B2). The plots are shifted vertically to improve clarity.

bcc (β_1) phase. In particular, it is interesting to notice that the highest characteristic peak of the $2H$ phase, $(1\ 2\ \bar{1})$, observed in the pattern of alloy A1, is replaced by $(1\ 2\ \bar{8})$ and $(1\ 2\ 10)$ peaks, characteristic of the $18R$ phase, in the pattern of alloy B1. This finding shows that samples with low ΔS transform to the $18R$ phase while samples with high ΔS transform to the $2H$ phase. It is worth noting that our results are in agreement with recent results by Kato *et al.*¹² who deduced $\Delta S = 1.31$ J/mol K for the bcc \rightarrow $18R$ transition and $\Delta S = 1.59$ J/mol K for the bcc \rightarrow $2H$ transition from strain-stress measurements.¹³

Since the martensitic structure is known to depend on the e/a value of the alloy system, an analysis of the e/a dependence of ΔS is worth performing. In order to obtain e/a as a function of the alloy composition, we have assumed, as usual,³ that each Cu atom contributes one electron and each Al atom three electrons. The situation is less clear for Mn atoms. For the class of alloys studied here it has been proposed¹⁴ that the contribution of Mn atoms is given by $(m/\mu_B - 3)$, where m is the magnetic moment of Mn atoms and μ_B is the Bohr magneton. From experimental data it has been deduced¹⁴ that m/μ_B is very close to 4, resulting in a contribution of one electron per Mn atom. The e/a ratios calculated for the alloys studied are listed in Table I. The measured ΔS values are plotted as a function of e/a in Fig. 3. A change in ΔS is observed for a value of e/a around 1.46. This result is in agreement with a passage from the $18R$ to the $2H$ structures at $e/a = 1.46$ observed by transmission electron microscopy (TEM).¹⁵ This value of e/a is very close to the value of e/a where the two phase boundaries of

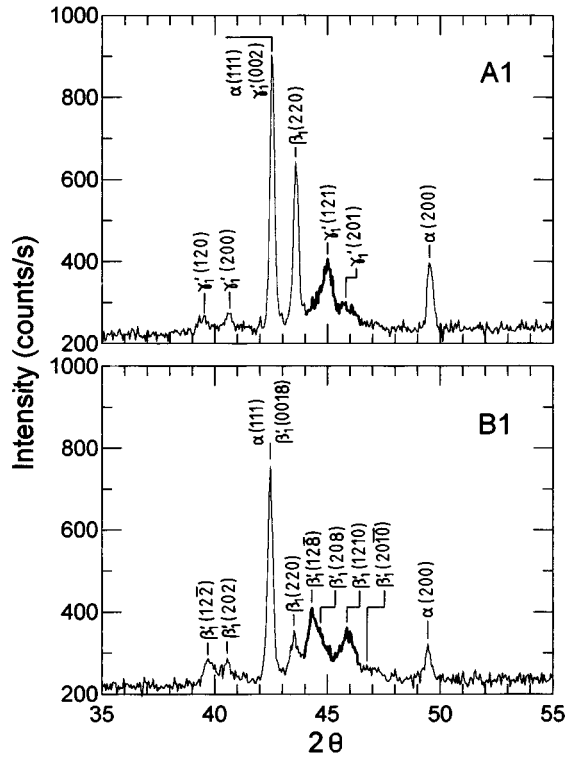


FIG. 2. Room-temperature powder diffractograms of alloys A1 and B1. The position of the peaks associated with the different phases is indicated. Note the difference between the $\gamma'_1(121)$ peak in diffractogram A1 and the $\beta'_1(128)$ and $\beta'_1(1210)$ peaks in diffractogram B1.

the bcc stability region meet each other (eutectoid point) in the equilibrium phase diagram of the two families studied,¹⁶ suggesting that the martensitic structure changes from 18R to 2H at a value of e/a very close to the value of the eutectoid point $(e/a)_{eu}$. In order to check if this idea can be extended to other Cu-based shape-memory alloys, we have collected from the literature a large number of data for different Cu-

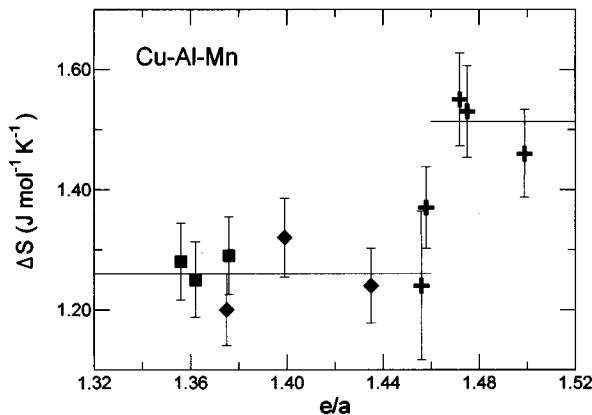


FIG. 3. Entropy difference between β and martensite as a function of electron concentration, from present experiments (+, $\text{Cu}_3\text{Al-Mn}$ line; \diamond , $\text{Cu}_3\text{Al-Cu}_3\text{Mn}_2$ line) and taken from M.O. Prado, P.M. Decorte, and F. Lovey, *Scr. Metall. Mater.* **33**, 877 (1995) (\square , $\text{Cu}_3\text{Al-Cu}_3\text{Mn}_2$ line). Solid lines: average values for $e/a \leq 1.45$ (β'_1 martensite) and for $e/a \geq 1.47$ (γ'_1 martensite), respectively.

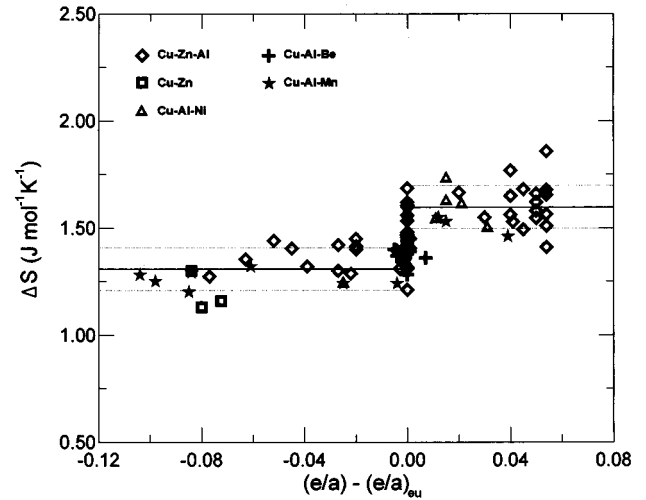


FIG. 4. Entropy differences for several Cu-based alloys, as a function of the reduced electron per atom ratio, $\alpha \equiv e/a - (e/a)_{eu}$. Data are collected from a large number of papers, and include the present results for Cu-Al-Mn. Solid lines are averages for $\alpha \leq -0.01$ and $\alpha \geq 0.01$, and dashed lines indicate, in each case, the corresponding standard deviation.

based alloys, and we have plotted them (including the present values for Cu-Al-Mn) in Fig. 4 as a function of $\alpha \equiv e/a - (e/a)_{eu}$. The $(e/a)_{eu}$ values are 1.48 for Cu-Zn-Al, 1.53 for Cu-Al-Ni, and 1.49 for Cu-Al-Be. It is clear from Fig. 4 that all ΔS values collapse on a single step function that changes from a value 1.31 ± 0.10 J/mol K to a value 1.60 ± 0.10 J/mol K at $\alpha = 0$. Systems with negative α transform to the 18R structure, while systems with positive α to the 2H one. At $\alpha = 0$ data spread over a large range of values; this reflects the fact that samples with compositions close to the eutectoid may transform into a mixture of the two phases.¹⁷ It has been recently proposed that ΔS is a linear function of e/a for Hume-Rothery alloys;¹⁸ the apparent discrepancy with the results presented here could arise from the fact that the different alloy families have different $(e/a)_{eu}$ values, and this can mask the scaling of ΔS because the jump will spread over a broad range of e/a . Our present results indicate a difference in entropy between the two close-packed structures of 0.3 ± 0.2 J/mol K, independent of the alloy system. It is worth mentioning that the values reported in the literature, evaluated from stress-strain measurements in a number of Cu-based alloys [$\Delta S^{18R \rightarrow 2H} = 0.2$ J/mol K (Ref. 19) and $\Delta S^{18R \rightarrow 2H} = 0.4$ J/mol K (Ref. 20) for Cu-Al-Ni; $\Delta S^{18R \rightarrow 2H} = 0.2$ J/mol K for Cu-Sn (Ref. 12) and $\Delta S^{18R \rightarrow 2H} = 0.3$ J/mol K for Cu-Al-Mn (Ref. 12)] are quite coincident with the value evaluated in this work.

The fact that ΔS values for Cu-Al-Mn coincide with ΔS values for other nonmagnetic Cu-based alloys leads us to conclude that a possible magnetic contribution to the overall entropy change would be very small. In agreement with this result we have found that the magnetic susceptibility jump at the martensitic transition is not influenced by an applied magnetic field ranging from 0 to 1 T.

From the results presented above, we conclude that the excess of entropy of the bcc phase in these systems arises

mainly from the vibrational degrees of freedom. Hence, the different value found for the entropy change between the bcc and different close-packed phases is a consequence of different densities of vibrational states for these close-packed phases.

Finally, it is interesting to recall that these alloys exhibit long-range configurational order. The entropy excess of the bcc phase could also depend on the degree of configurational order, in addition to its dependence on the particular martensitic structure. Such a dependence has been found to be negligible for Cu-Zn-Al,²¹ in agreement with the fact that the fundamental structure of the close-packed phase is not modified by configurational order. Moreover, recent specific heat measurements²² have shown (within the experimental uncertainties) that the vibrational contribution to the entropy of the high-temperature bcc phase is also independent of atomic ordering. Thus, we conclude that this same result must hold for the entropy of the close-packed phase. Finally we point out that, in contrast with other alloy systems like Ni₃Al or Fe₃Al,⁴ configurational order has little influence on the vibrational entropy of Cu-based Hume-Rothery alloys.

IV. SUMMARY AND CONCLUSIONS

In this paper we have studied the Cu-Al-Mn shape-memory alloy. 18R and 2H martensitic phases form for $e/a < (e/a)_{eu}$ and $e/a > (e/a)_{eu}$, respectively; here $(e/a)_{eu}$ is the value of e/a corresponding to the composition for which the bcc phase is stable in the largest temperature range. Such an e/a dependence of the resulting martensitic structure

could be reminiscent of the dependence of the equilibrium phases on the electron concentration. This is in agreement with the fact that the relative phase stability of equilibrium bcc and fcc structures has been recently predicted using thermodynamic data corresponding to the martensitic transition.¹⁸

Here we have found that the entropy change at the martensitic transition depends solely on the resulting close-packed structure, and, from the analysis of published data, this result has been shown to be general for Cu-based shape-memory alloys. In particular it has been shown that the entropy change for a given close-packed structure is always the same for all the alloys analyzed. We obtain that $\Delta S = 1.31 \pm 0.10$ J/mol K for the transition to the 18R phase, and $\Delta S = 1.60 \pm 0.10$ J/mol K for the transition to the 2H phase. This excess of entropy of the bcc phase arises from the vibrational degrees of freedom. Hence, the different excesses of entropy for the different close-packed phases are a consequence of different densities of vibrational states in the different close-packed structures. To our knowledge, no experimental data for the density of states in the martensitic phase are available at present to confirm this point directly.

ACKNOWLEDGMENTS

This work has received financial support from the CICYT (Spain), Project No. MAT95-0504, and from the CIRIT (Catalonia), Project No. SGR119. E.O. acknowledges financial support from DGICYT (Spain).

¹W. Petry, J. Phys. (France) IV, Colloq. **5**, C2-15 (1995).

²L. Delaey, in *Phase Transformations in Materials, Vol. 5 of Materials Science and Technology*, edited by P. Haasen (VCH, Weinheim, 1991), p. 339.

³T. B. Massalski and U. Mizutani, Prog. Mater. Sci. **22**, 151 (1978).

⁴L. Anthony, J. K. Okamoto, and B. Fultz, Phys. Rev. Lett. **70**, 1128 (1993); L. Anthony, L. J. Nagel, J. K. Okamoto, and B. Fultz, *ibid.* **73**, 3034 (1994).

⁵M. Ahlers, Prog. Mater. Sci. **30**, 135 (1986).

⁶Ll. Mañosa, A. Planes, J. Ortín, and B. Martínez, Phys. Rev. B **48**, 3611 (1993).

⁷E. Obradó (unpublished results).

⁸G. Guénin *et al.*, *Proceedings of ICOMAT'86* (The Japan Institute of Metals, Nara, 1986), p. 794.

⁹Sample A5 transforms in a temperature range close to the lower limit of our experimental system. This results in a larger experimental error in ΔS , arising from the difficulty in determining a proper calorimetric base line.

¹⁰A. Planes, J. L. Macqueron, M. Morin, G. Guénin, and L. Delaey, J. Phys. (France) Colloq. **43**, C4-615 (1982).

¹¹During powder preparation it is not possible to inhibit the growth of precipitated phases (α and γ) which are always present in different amounts depending on the composition of the specific

alloy. Their characteristic peaks are clearly observable in the diffractograms of Fig. 2.

¹²H. Kato and S. Miura, Acta Metall. Mater. **43**, 351 (1995); H. Kato, J. Dutkiewicz, and S. Miura, *ibid.* **42**, 1359 (1994).

¹³In stress-strain experiments, the entropy change is obtained from the temperature dependence of the resolved shear stress at which the transition takes place (Clausius-Clapeyron equation). In a given sample, the transition to the 2H phase is observed at low stress values, while the transition to the 18R phase takes place at higher stress values.

¹⁴B. Caroli and A. Blandin, J. Phys. Chem. Solids **27**, 503 (1966).

¹⁵J. M. Guilemany, F. Peregrin, F. C. Lovey, N. Llorca, and E. Cesari, Mater. Characterization **26**, 23 (1991).

¹⁶J. J. Conioux, J. L. Macqueron, M. Robin, and J. M. Scarabello Scr. Metall. **22**, 821 (1988).

¹⁷J. van Humbeeck *et al.*, Trans. Jpn. Inst. Met. **28**, 383 (1987).

¹⁸M. Ahlers, Z. Phys. B **99**, 491 (1996).

¹⁹K. Otsuka, C. M. Wayman, K. Nakai, H. Sakamoto, and K. Shimizu, Acta Metall. **24**, 207 (1976).

²⁰J. Ortín, Ll. Mañosa, C. M. Friend, A. Planes, and M. Yoshikawa, Philos. Mag. A **65**, 461 (1992).

²¹A. Planes, J. L. Macqueron, R. Rapacioli, and G. Guénin, Philos. Mag. A **61**, 221 (1990).

²²Ll. Mañosa and A. Planes (unpublished results).